# Near-Infrared Absorbing Squaraine Dyes for Solar Cells: Relationship between Architecture and Performance

Zhengquan Yan, Shanyi Guang,* Xinyan Su, and Hongyao Xu*

College of Material Science and Engineering & State Key Laboratory for Modification of Chemical Fibers and Polymer Materials, College of Chemistry & Biology Engineering, Donghua University, Shanghai 201620, China

ABSTRACT: To further investigate the influence of dye architecture on dye-sensitized solar cell (DSSC) performance, some near-infrared absorbing quinoline-based squaraine dyes (**4a**, **4b**, and **4c**) with different conjugated degrees carrying carboxylic or sulfonic groups as anchoring groups were designed, prepared, and applied as sensitizers in solar cells. The photophysical and photochemical studies showed that photoelectric conversion efficiencies (η) are significantly affected by molecular structures; i.e., η of **4c** with the strongest polarity and anchoring ability and the longest π electron conjugated degree was two times more than that of **4b** and six times more than that of **4a**. That is, the molecules with smaller optical band gap and higher molar absorption coefficient will possess better light-harvesting properties and enhanced conversion efficiency. Furthermore, all excited state orbitals relevant for the $\pi-\pi$ electron transition both in **4b** and **4c** are delocalized over the anchoring groups, ensuring a strong electronic coupling to the conduction band of TiO$_2$ and hence a fast electron transfer.
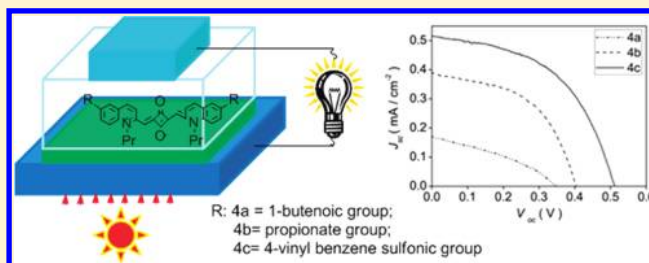
1. INTRODUCTION

It is well-known that environmental concerns and the finite nature of fossil fuels have led to great interest and growing development in the field of renewable energy sources. The annual energy input of solar irradiation on Earth (5% UV, 43% visible, 52% IR) is a huge 3.78×10^{24} J, exceeding the world's yearly energy consumption by several thousand times.[1,2] Harnessing the abundant energy not only can easily compensate for our world energy needs but also is clean without contaminating humankind. Solar energy conversion is one of the most promising ways to resolve the energy crisis.[3−5] The dye-sensitized solar cell (DSSC) is an effective device to convert solar energy into electron energy directly and has been attracting considerable attention since the pioneering work in 1991.[6] Although the most successful charge transfer sensitizers employed for DSSCs are ruthenium polypyridyl complexes,[3,7−9] the disadvantages of ruthenium complexes such as limited ruthenium resources, heavy-metal toxicity, difficulty of purification, and stability issues still limit the large-scale applications of this type of solar cells.[10]

As an alternative to Ru complexes, metal-free organic dyes have also been utilized as sensitizers of DSSCs because they have advantages such as the high molar absorption coefficient, wide absorption bands, facile molecular design, and lack of concern with the noble metal resource.[11−14] Among all the metal-free organic dyes identified, squaraine dyes are a particularly promising class of dyes widely applied in solar cells because of the ultrastrong absorption properties ($\varepsilon \geq 10^5$ L·mol^{-1}·cm^{-1}) from red to near-IR regions.[15−19] Yum et al.[20] reported that a solar cell sensitized by an asymmetric far-red absorbing indole-based squaraine dye could achieve high conversion efficiency (η = 4.5%) originating from the

unidirectional flow of electrons from the light-harvesting components of the sensitizer to the semiconductor surface. Maeda et al.[21] developed a novel class of near-infrared absorbing squarylium sensitizers with linearly extended π-conjugated structures, which exhibited not only a remarkable response in the near-infrared (NIR) region over 750 nm but also a panchromatic response. In 2012, Fu et al.[10] designed a novel squaraine molecule with no diradical character or small contribution of the diradicaloid component to resonance, which might open a new possibility for the improvement of the photovoltaic performance through a judicious design on squaraine dyes. However, the performances of DSSCs based on organic dyes are still poor and have not yet exceeded those based on Ru complexes owing to high electron recombination and low electron transfer rate.[22,23] Therefore, how to optimize dye-molecular structure, improve the solar-to-electric conversion efficiency, and increase the price−performance ratio at the same time remains to be a big challenge.

In this article, we designed and synthesized a series of near-infrared absorbing squaraine dyes (**4a**, **4b**, and **4c**) with different anchoring groups and π-electron-conjugated degrees and systematically studied the influence of molecular structures, especially the polarity, anchoring ability, and conjugated degree of dye molecules on their photophysical, photochemical, and electrochemical properties of dyes and their sensitizing solar-cell performances.
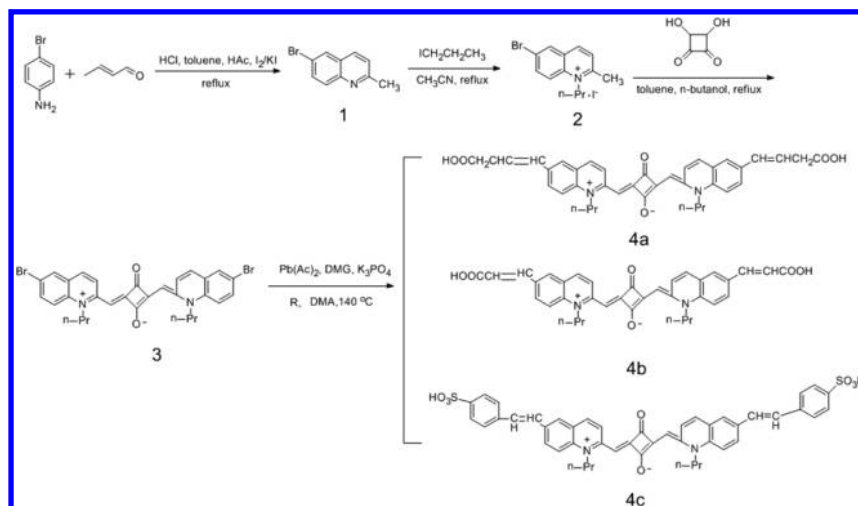
Scheme 1. Synthetic Routes of the Target Quinoline-Based Squaraine Dyes (4a, 4b, and 4c)

2. EXPERIMENTAL SECTION

2.1. Materials and Measurements. 4-Vinylbenzenesulfonic acid, 3-butenoic acid, propionate, 1-iodopropane, and palladium acetate were purchased from Aldrich. *N,N*-dimethylglycine (DMG) was prepared according to the reported procedure in the literature. All the other chemicals were of analytical reagent grade and purchased from Shanghai Chemical Reagent Company. All the reagents were used directly as received without any further purification except that *N*-methylpyrrolidone and crotonaldehyde were distilled immediately prior to use. The electrolyte solution was a mixture of DMPII/LiI/I$_2$/TBP/GuSCN, and the TiO$_2$ electrode and Pt counter electrode with 0.25 cm^2 working area were purchased from Dalian HeptaChroma SolarTech Co., Ltd. Water used throughout was doubly deionized.

FT-IR spectra were recorded as KBr pellets on a Perkin-Elmer Model 882 infrared spectrometer scanning from 4000 to 500 cm^{-1}. ^{1}H NMR spectra were recorded using a Bruker AMX-500 spectrometer operating at 400 MHz, with tetramethylsilane (TMS) as the reference and DMSO-d_6 as solvent. Elemental analyses were conducted with an Elemental Vario EL-III apparatus. UV–vis spectra were recorded on a Lambda 35 UV/vis spectrometer using a 1 cm square quartz cell. Cyclic voltammetry (CV) measurements were carried out in a three-electrode measuring device with a glassy carbon working electrode, a Pt wire counter electrode, a Hg/Hg$_2$Cl$_2$ reference electrode, and a supporting electrolyte of 0.1 M TBAP in DMSO. The photovoltaic performance of the device was recorded on a CIMPS-1 electrochemical workstation under AM 1.5 G solar irradiation (100 mW/cm^2). All the theoretical calculations were implemented in the Gaussian 03 suite of program.[24]

2.2. Synthesis. The target NIR absorbing quinoline-based squaraine dyes **4a**, **4b**, and **4c**, carrying carboxylic or sulfonic groups as anchoring groups with different conjugated degrees, were prepared according to Scheme 1.

2.2.1. Preparation of 6-Bromoquinaldine (1). To a 100 mL three-necked bottle was added hydrochloride (44.8 mL, 6 mol/L), 4-bromoaniline (1535 mg, 8.9 mmol), and acetic acid (0.5 mL, 8.9 mmol). The formed mixture was refluxed at 100 °C for 0.5 h, followed by addition of iodine/potassium (50 mg/132 mg, 0.4 mmol/0.8 mmol) and 10 mL of toluene. Then a mixture of toluene (2 mL) and crotonaldehyde (1.5 mL, 17.8

mmol) was added dropwise over a period of 1 h and refluxed for another 6 h. The reaction mixture was cooled to room temperature, adding ammonia solution to alkalinity to precipitate the product. The precipitation was filtered and purified by column chromatography on silica gel (eluent: petroleum ether/ethyl acetate = 1:6) to afford 1.76 g (89%) 6-bromoquinaldine **1**.

IR (KBr), ν_{max}: 3048 (C−H), 1596, 1488, 1463 (Ar), 637 cm^{-1} (C−Br). ^{1}H NMR (400 Hz, DMSO-d_6, RT, TMS) δ: 7.97 (d, J = 8.4 Hz, 1 H, H^4), 7.90 (s, 1 H, H^5), 7.76 (d, J = 7.4 Hz, 1 H, H^8), 7.74 (d, J = 7.0 Hz, 1 H, H^3), 7.31 (d, J = 8.8 Hz, 1 H, H^5), 2.74 (s, 3 H, CH$_3$). Anal. Calcd. for C$_{10}$H$_8$NBr: C, 50.08; H, 3.63; N, 6.03. Found: C, 60.17; H, 3.77; N, 6.14.

2.2.2. Preparation of N-propyl-6-bromoquinaldinium salt (2). A mixture of **1** (666 mg, 3 mmol), propyl iodide (1.7 g, 10 mmol), and 2 mL of acetonitrile was heated in a sealed tube at 100−105 °C for 12 h. The precipitate formed was filtered, washed thoroughly with cold diethyl ether, and purified by column chromatography on silica gel (eluent: petroleum methanol/chloroform =1:4) to afford 0.72 g (61%) of *N*-propyl-6-bromoquinaldinium salt **2**.

IR (KBr), ν_{max}: 3019, 2956, 2870 (C−H), 1601, 1509, 1466 (Ar), 598 cm^{-1} (C−Br). ^{1}H NMR (400 Hz, DMSO-d_6, RT, TMS) δ: 8.68 (d, J = 8.2 Hz, 1 H, H^4), 8.53 (d, J = 8.5 Hz, 1 H, H^3), 8.35 (s, 1 H, H^5), 8.05 (d, J = 5.7 Hz, 1 H, H^8), 7.83 (d, J = 8.5 Hz, 1 H, H^5), 3.98 (t, J = 7.7 Hz, 2 H, C*H*$_2$CH$_2$CH$_3$), 2.84 (s, 3 H, CH$_3$), 1.91 (m, J = 7.5 Hz, 2 H, CH$_2$C*H*$_2$CH$_3$), 1.15 (t, J = 2.9 Hz, 3H, CH$_2$CH$_2$C*H*$_3$). Anal. Calcd. for C$_{13}$H$_{14}$NBrI: C, 39.93; H, 3.61; N, 3.58. Found: C, 40.03; H, 3.67; N, 3.54.

2.2.3. Preparation of 6-Bromoquinaldine Squaraine Dye (3). A mixture of **2** (784 mg, 2 mmol), squaric acid (114 mg, 1 mmol), and quinoline (1 mL) was refluxed in a mixture of *n*-butanol and toluene at the ratio of 1:1 (v/v, 15 mL) with azeotropic distillation of water for 24 h. The solvent was distilled off under reduced pressure to obtain a residue which was purified by column chromatography on silica gel (eluent: methanol/chloroform = 1:9) to afford 1.48 g (86%) of 6-bromoquinaldine squaraine dye **3**.

IR (KBr), ν_{max}: 3016, 2953, 2872 (C−H), 1616, 1581, 1449 cm^{-1} (Ar), 1317, 1248 (O−C−O), 596 (C−Br). ^{1}H NMR (400 Hz, DMSO-d_6, RT, TMS) δ: 9.56 (d, J = 5.7 Hz, 2 H, H^4), 9.30 (d, J = 6.4 Hz, 2 H, H^9), 8.63 (d, J = 9.2 Hz, 2 H, H^3), 8.50

(d, J = 8.0 Hz, 2 H, H[8]), 8.30 (s, 2 H, H[5]), 8.07 (d, J = 7.8 Hz, 2 H, H[7]), 4.49 (t, J = 7.5 Hz, 4 H, CH_2CH$_2$CH$_3$). 1.95 (m, J = 7.5 Hz, 4 H, CH$_2$CH_2CH$_3$), 0.95 (t, J = 2.6 Hz, 6 H, CH$_2$CH$_2$CH_3). Anal. Calcd. for C$_{30}$H$_{27}$N$_2$Br$_2$O$_2$: C, 59.33; H, 4.48; N, 4.61. Found: C, 59.24; H, 4.57; N, 4.69.

2.2.4. Preparation of the Target-Functionalized NIR Squaraine Dyes (4a, 4b, and 4c). The target-functionalized NIR squaraine dyes were prepared using **3** and different vinyl derivatives as raw materials with 1:2 molar feed ratio, by a conventional Heck reaction between C–Br and C=C using Pb(Ac)$_2$ as a catalyst, anhydrous K$_3$PO$_4$ as an acid-binding agent, and DMG as a ligand at ca. 130 °C in dry *N*-methyl pyrrolidone under nitrogen atmosphere.

Taking the synthesis of **4a** as an example, a mixture of **3** (121 mg, 0.2 mmol), 3-butenoic acid (36 mg, 0.44 mmol), DMG (123 mg, 1.2 mmol), palladium acetate (16 mg, 0.06 mmol), and K$_3$PO$_4$ (127 mg, 0.6 mmol) was placed in a 50 mL sealed three-necked bottle, and the bottle was evacuated under vacuum and then flushed with dry nitrogen three times. After 5 mL of fresh distilled *N*-methyl pyrrolidone was injected in, the reaction mixture was refluxed at 130 °C under nitrogen for 40 h and then cooled to room temperature. The mixture was then added into 100 mL of 0.1 mol·L^{-1} NaOH and filtered after standing for ca. 1 h. The filtrate was added dropwise into 100 mL of dilute hydrochloric acid to precipitate the dye. The precipitation redissolved in reasonable NaOH, and the solution was added dropwise into dilute hydrochloric acid to precipitate the dye. This purification procedure was repeated three times. The last filter was vacuum dried to constant at ca. 40 °C to get the crystal **4a** in the yield of 53%.

IR (KBr), ν_{max}: 3386–2500 (–COOH), 1726 (C=O), 1611, 1551, 143 856 cm^{-1} (Ar). ^{1}H NMR (400 Hz, DMSO-d_6, RT, TMS) δ: 12.14 (s, 2 H, COOH), 9.434 (d, J = 6.2 Hz, 2 H, H[4]), 9.32 (d, J = 6.2 Hz, 2 H, H[9]), 8.69 (d, J = 7.7 Hz, 2 H, H[3]), 8.53 (d, J = 7.7 Hz, 2 H, H[8]), 8.35 (s, 2 H, H[5]), 8.10 (d, J = 7.8 Hz, 2 H, H[7]), 6.32 (s, 4H, CH=CH), 4.95 (t, J = 7.5 Hz, 4 H, CH_2CH$_2$CH$_3$), 3.28 (d, 4 H, CH_2COOH), 1.92 (m, J = 7.1 Hz, 4 H, CH$_2$CH_2CH$_3$), 0.96 (t, J = 7.1 Hz, 6 H, CH$_2$CH$_2$CH_3). Anal. Calcd. for C$_{38}$H$_{36}$N$_2$O$_6$: C, 74.00; H, 5.88; N, 4.54. Found: C, 73.98; H, 5.91; N, 4.57.

4b was prepared as above from **3** and propionate in the yield of 49%.

IR (KBr), ν_{max}: 3415–2500 (–COOH), 1703 (C=O), 1613, 1548, 1438 cm^{-1} (Ar). ^{1}H NMR (400 Hz, DMSO-d_6, RT, TMS) δ: 12.78 (s, 2 H, COOH), 9.55 (d, J = 5.9 Hz, 2 H, H[4]), 9.31 (d, J = 6.2 Hz, 2 H, H[9]), 8.70 (d, J = 7.8 Hz, 2 H, H[3]), 8.51 (d, J = 7.6 Hz, 2 H, H[8]), 8.38 (s, 2 H, H[5]), 8.06 (d, J = 7.7 Hz, 2 H, H[7]), 6.73 (s, 4H, CH=CH), 5.07 (t, J = 7.5 Hz, 4 H, CH_2CH$_2$CH$_3$), 1.95 (m, J = 7.5 Hz, 4 H, CH$_2$CH_2CH$_3$), 0.92 (t, J = 7.6 Hz, 6 H, CH$_2$CH$_2$CH_3). Anal. Calcd. for C$_{36}$H$_{32}$N$_2$O$_6$: C, 73.45; H, 5.45; N, 4.76. Found: C, 73.42; H, 5.47; N, 4.79.

4c was prepared as above from **3** and 4-vinylbenzene sulfonic acid in the yield of 47%.

IR (KBr), ν_{max}: 3433–2400 (–SO$_3$H), 1696 (C=O), 1624, 1600, 1588 cm^{-1} (Ar), 1168 (S–O). ^{1}H NMR (400 Hz, DMSO-d_6, RT, TMS) δ: 12.07 (s, 2 H, SO$_3$H), 9.60 (d, J = 7.9 Hz, 2 H, H[4]), 9.46 (d, J = 7.8 Hz, 2 H, H[9]), 8.80 (d, J = 7.5 Hz, 2 H, H[3]), 8.54 (d, J = 7.7 Hz, 2 H, H[8]), 8.33 (s, 2 H, H[5]), 8.12 (d, J = 7.5 Hz, 2 H, H[7]), 6.12–7.16 (m, 12 H, CH=CH, ph), 5.03 (t, J = 4.5 Hz, 4 H, CH_2CH$_2$CH$_3$), 1.96 (m, J = 4.6 Hz, 4 H, CH$_2$CH_2CH$_3$), 0.91 (t, J = 4.6 Hz, 6 H, CH$_2$CH$_2$CH_3).

Anal. Calcd. for C$_{46}$H$_{40}$N$_2$S$_2$O$_8$: C, 67.96; H, 4.96; N, 3.45. Found: C, 69.87; H, 4.97; N, 3.49.

3. RESULTS AND DISCUSSION

3.1. Synthesis. The target functional NIR absorbing squaraine dyes (**4a**, **4b**, and **4c**) were prepared using **3** and different vinyl derivatives as raw materials through a conventional Heck reaction between C–Br and C=C bond according to the literature.[17,25] To avoid the byproduct water, which can deactivate the catalyst to lower the Heck addition yield, anhydrous K$_3$PO$_4$ was selected as an acid-binding agent instead of anhydrous K$_2$CO$_3$.

The target functional dyes and their intermediates were characterized by IR, ^{1}H NMR, and elemental analysis, and satisfactory analytic data corresponding to their molecular structures were obtained. All the characteristic data were given in section 2.2.

3.2. Optical Properties—UV–Vis Spectroscopy. UV–vis spectra of the squaraine dyes **4a**, **4b**, and **4c** in DMSO with concentrations of 1.5×10^{-6} mol·L^{-1} are provided in Figure 1.
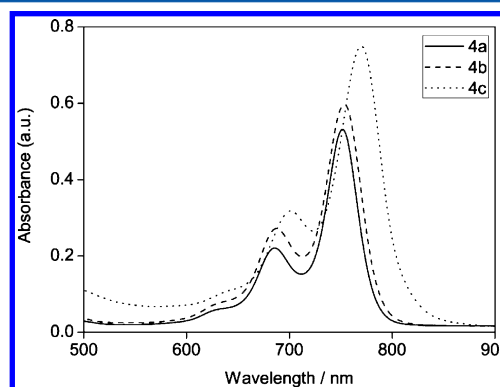

Figure 1. UV–vis absorbance spectra of dyes **4a**, **4b**, and **4c** in DMSO (c = 1.5×10^{-6} mol·L^{-1}).

Owing to their similar structure, all the squaraine dyes studied in this work have the same UV–vis absorbing spectral profiles and exhibit a similar maximum π–π* electron transition peak located in the range of 650–800 nm. But as a consequence of the extended π system of the dye molecules, its absorption maximum is slightly red-shifted from 750 nm for **4a** to 754 nm for **4b** further to 770 nm for **4c**, respectively. Furthermore, the corresponding molar absorption coefficients (ε_{max}) for **4a**, **4b**, and **4c** are 3.53×10^5, 3.73×10^5, and 5.0×10^5 L·mol^{-1}·cm^{-1}, respectively, increasing with the polarity and molecular conjugated degree, i.e., 4-vinylbenzene sulfonic group > propionate group > 1-butenoic group. The very high molar absorption coefficients of the functional dyes allow using thinner nanocrystalline TiO$_2$ films for the photoanodes of DSCCs.

Remarkably, the optical band gaps (E_g^{opt}) of **4a**, **4b**, and **4c**, determined from the onset absorption edge (λ_g^{opt}) at higher wavelengths (5% λ_{max}), are 1.54, 1.53, and 1.47 eV, respectively, according to the formula 1[26]

$$E_g^{opt}(ev) = h\nu/\lambda_{onset}^{abs} = 1240/\lambda_{onset}^{abs} \qquad (1)$$

It is clearly drawn that, with increase of molecular conjugated degree and polarity of terminal-substituted groups, squaraine dye molecules show better π electrons delocalizability and

lower band gap energy, which facilitates intermolecular charge transfers (ICT) in the excited state.

3.3. Electrochemical Properties—Cyclic Voltammetry (CV).
It is reported that the oxidation potentials of the ground and excited states of the dyes for DSSCs, which are usually replaced by HOMO and LUMO, must match with the energy levels of I^-/I_3^- redox potential and E_{CB} of TiO$_2$ electrode, respectively.[27] So the electrochemical properties of **4a**, **4b**, and **4c** were measured to determine the energy levels of HOMO and LUMO combining with their UV−vis spectra.

CV was carried out in a three-electrode measuring device with a glassy carbon working electrode, a Pt wire counter electrode, a Hg/Hg$_2$Cl$_2$ reference electrode, and a supporting electrolyte of 0.1 M TBAP in DMSO, which was degassed with N$_2$ for 20 min prior to scanning with a scan rate of 100 mV/s (Figure 2).
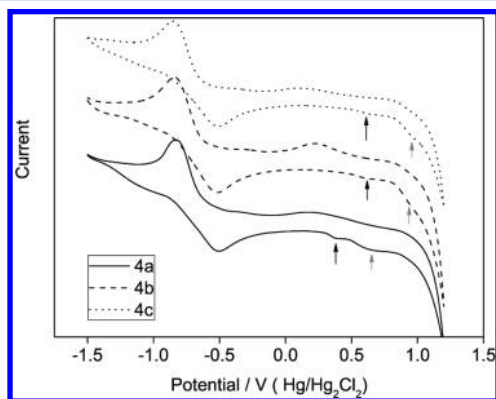

Figure 2. Cyclic voltammetry plots of the dyes **4a**, **4b**, and **4c** (scan rate 100 mV/s).

The outset oxidation potentials (E_{ox}) of **4a**, **4b**, and **4c** are 0.608, 0.858, and 0.852 V (vs NHE), respectively, which are all larger than the oxidation potential (E_{ox}) of I/I_3^- (~0.4 V vs NHE), enough to provide the necessary driving force for the regeneration of the oxidized dye.[27] According to the literature,[26,27] the onset oxidation potentials in the cyclic voltammogram were taken as the HOMO, and the LUMO is estimated by subtracting the value of the optical band gap (λ_g^{opt}) from the HOMO. The HOMO energy levels of **4a**, **4b**, and **4c** are 0.608, 0.858, and 0.852 V, and the LUMO energy levels are −0.932, −0.672, and −0.618 V, respectively, which are all lower than the conduction bond energy level (E_{CB}) of the TiO$_2$ electrode (−0.5 V vs NHE); i.e., the electrons in the excited dyes have enough driving force to inject into the conduction band of the TiO$_2$ electrode.[27]

3.4. Computational Analysis of Dye Structure and Electron Distribution.
To validate the rationality of the structural design of dye molecules, theoretical calculation was conducted under the Gaussian 03 software suite with the B3LYP/6-31G level of theory.[24] The optimized geometries and electron cloud density distributions of **4a**, **4b**, and **4c** are shown in Figure 3 and Figure 4, respectively.

It is striking to find from Figure 3 that the basic unit of squaraine is rigid and planar in which electrons are more delocalized and even, and so the absorption intensity is ultrastrong ($\varepsilon \geq 10^5$ L·mol^{-1}·cm^{-1}) and the absorption wavenumber red-shifts to the NIR region ($\lambda_{max} > 750$ nm). However, the overall molecular conjugated degrees change greatly once combined with different substituents. For example,
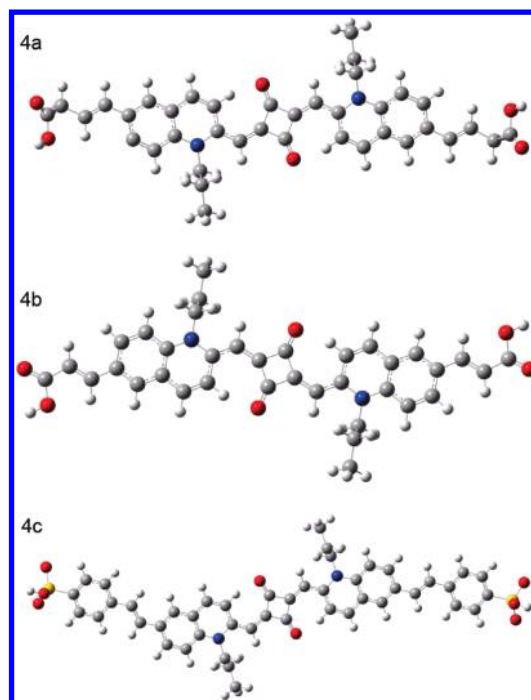

Figure 3. Optimized geometries of dyes **4a**, **4b**, and **4c**. O, N, C, and H atom are represented as red, blue, gray, and white-gray, respectively.

owing to the fact that the frameworks of squaraine and the substitutes in both **4b** and **4c** were connected through $\pi-\pi$ double bonds, the molecules were rigid and planar and so valence electrons were distributed evenly over the whole molecular, which allows efficient vectorial electron transfer from the excited light-harvesting dye toward the semiconductor surface. But for **4a**, the π-framework and the substitutes were isolated by two C−C single bonds, so the overall molecular conjugated degree and planarity decrease, which make it difficult for excited electrons to delocalize to the substituent group and further to the semiconductor surface; i.e., poorly vectorial electron transfer efficiency was shown from the light-harvesting dye toward the semiconductor surface.

On closer inspection of the electronic cloud density distribution of **4a**, **4b**, and **4c** shown in Figure 4, the electronic clouds in the HOMO−1 of **4a**, **4b**, and **4c** are all localized within the molecular core, even in the HOMO delocalized in π framework without the substituent groups. In the LUMO, there is a notable electron density contribution among the carboxylic group of **4b** or benzene sulfonic group of **4c**. Further in the LUMO+1, the electron cloud is localized completely within the substituent groups of both **4b** and **4c**. It means that a HOMO−LUMO excitation of **4b** and **4c** dyes can move the excited electron from the $\pi-\pi^*$ framework toward the anchor group and further to the semiconductor surface, which results in direct electron transfer. In contrast, for the dye **4a**, there is no electron contribution distributed at the carboxylic acid group even in the LUMO+1 excited state owing to the πframework and the terminal substituent group being isolated by two C−C single bonds; i.e., the excited electron cannot efficiently transfer from the excited dyes to the conduction band of the TiO$_2$ electrode.[26]

E_g^{calc} values calculated from the B3LYP/6-31G level of theory are shown in Table 1. The E_g^{calc} values of **4a**, **4b**, and **4c** are 1.84, 1.73, and 1.68 eV, respectively, which are all higher than the experimental E_g^{opt}, but exhibit the order of **4a** > **4b** > **4c** with
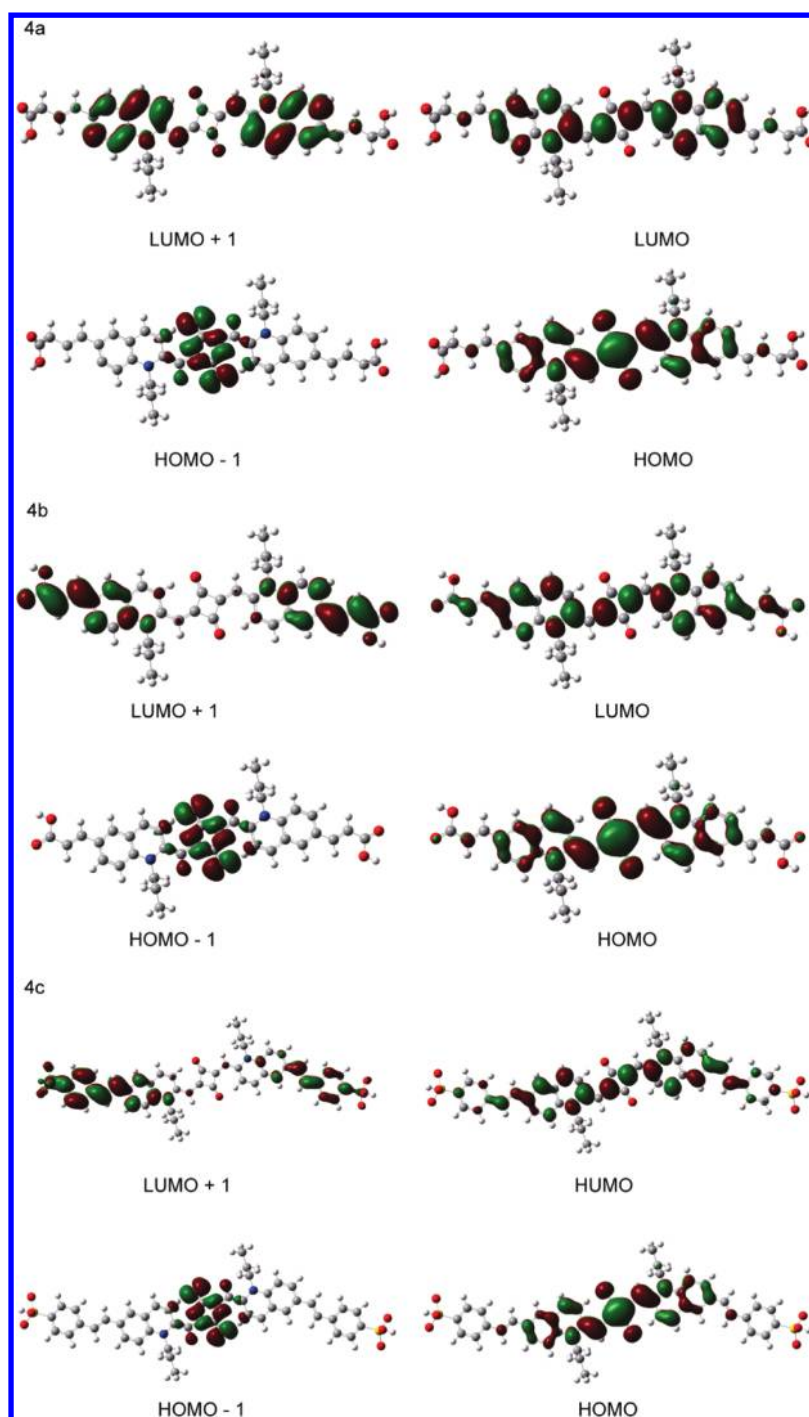
Figure 4. Electronic cloud density distribution of target squaraine dyes **4a**, **4b**, and **4c**.

increasing electronegativity and conjugated degrees of molecules. The differences between E_g^{opt} and E_g^{calc} may be owing to the fact that the orbital approximation is being used in theoretical calculation besides its basic assumption that all the calculated atoms exist in vacuum. The optical band gap is related to the difference between ground and excited state energies, not to the HOMO−LUMO energy gap.

Theoretical calculation results show that the excited electrons of **4b** and **4c** π frameworks can easily delocalize to the anchor groups, substituent carboxylic, or sulfonic group owing to their planar conjugated structures, which results in high electron transfer rate, low electron recombination, and an improved overall photovoltaic efficiency, vice versa, e.g., **4a**.

3.5. Preparation and Characterization of DSSC. To further confirm the influence of the dye structures on the performances of DSSCs, the DSSCs were composed of a dye-

Table 1. Calculation Electrochemical Properties of 4a, 4b, and 4c

	HOMO/eV	LUMO/eV	E_g^{calc}/eV
4a	−4.42	−2.58	1.84
4b	−4.37	−2.64	1.73
4c	−4.40	−2.72	1.68

adsorbed TiO_2 electrode, Pt counter electrode, and an organic electrolyte, i.e., a mixture of DMPII/LiI/I_2/TBP/GuSCN. Both TiO_2 working electrode and Pt counter electrode with 0.25 cm² working area were activated for 30 min at 450 °C, and then the TiO_2 electrodes were immersed in 1.0×10^{-4} mol·L⁻¹ solutions of **4a**, **4b**, and **4c** at room temperature overnight, rinsed several times with ethanol, and dried under N_2 atmosphere. After that the Pt counter electrode was placed on the TiO_2 electrode face to face, and between both the electrodes a drop of DMPII/LiI/I_2/TBP/GuSCN solution was injected. The DCCS was fixed and sealed with HY-914 resin, and the photovoltaic performance was recorded under AM 1.5 G solar irradiation (100 mW/cm²).

The experimental results are shown in Figure 5 and Table 2. From Figure 5, it can be easily found that, under the same
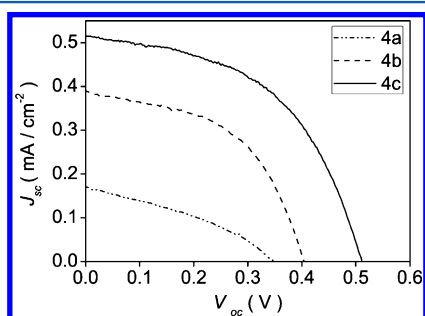

Figure 5. *I–V* curves of DSSCs sensitized with **4a**, **4b**, and **4c**, respectively.

Table 2. Photovoltaic Performances of DSSCs Sensitized with 4a, 4b, and 4c, Respectively (AM 1.5, 100 mW·cm⁻²)

sensitizers	J_{sc}/mA·cm⁻²	V_{oc}/V	ff	η/%
4a	0.51	0.35	0.24	0.07
4b	1.16	0.40	0.52	0.24
4c	1.54	0.51	0.51	0.40

conditions (TiO_2 as a working electrode, Pt counter electrode, organic electrolyte, and standard global AM 1.5 solar), the DSSC sensitized with **4c** has the best photovoltaic performance with J_{sc} (the highest short-circuit photocurrent density) of 1.54 mA·cm⁻², V_{oc} (the open-circuit voltage) of 0.51 V, and ff (the fill factor) of 0.51, while the DSSC sensitized by **4a** has the lowest performance with J_{sc} of 0.51 mA·cm⁻², V_{oc} of 0.35 V, and ff of 0.24. Derived from $\eta = J_{sc} \cdot V_{oc} \cdot ff / I_0$, where I_0 is the incident photon flux, the overall conversion efficiency (η) for DSSCs sensitized by **4c**, **4b**, and **4a** are 0.40, 0.24, and 0.07, respectively. η for the DSSC with **4c** is improved by six times compared to that with **4a** and by two times compared to that with **4b**, confirming that the photovoltaic performance of DSSCs increases with improving the polarity and anchoring ability of the substituents, the planarity and conjugated degree of the whole molecule, and the molar absorbance coefficient.

4. CONCLUSION

In conclusion, three kinds of squaraine derivatives (**4a**, **4b**, and **4c**) combined with different polar and anchoring group and conjugated degree substituents were prepared, characterized, and applied as sensitizers for DSSCs. It is clearly found from both theoretical and experimental results that the solar-to-electric conversion performance is improved with increasing polarity and conjugated degree of anchoring groups, in the

order of **4c** > **4b** > **4a**. The UV−vis spectroscopy, cyclic voltammetry, and theory calculations were used to investigate the influence of the dye molecular structure on the overall conversion efficiency η. It is found that the sensitizer dyes with stronger anchoring group, larger conjugated system, and stronger polarity will be beneficial to the conversion efficiency for DSSCs owing to the increase of the driving force for photoinduced electron injection and reduction of electron recombination probability.

■ AUTHOR INFORMATION

Corresponding Author
*Tel.: +8621 67792874. E-mail: syg@dhu.edu.cn (S.G.), hongyaoxu@163.com (H.X.).

Notes
The authors declare no competing financial interest.

■ REFERENCES

(1) Dieter, W.; Dieter, M. *Adv. Funct. Mater.* **1991**, *3*, 129−138.
(2) Robertson, N. *Angew. Chem., Int. Ed.* **2008**, *47*, 1012−1014.
(3) Wang, P.; Zakeeruddin, S. M.; Moser, J. E.; Nazeeruddin, M. K.; Sekiguchi, T.; Gratzel, M. *Nat. Mater.* **2003**, *2*, 402−407.
(4) Ho, K. C.; Wu, S. J.; Chen, C. Y.; Chen, J. G.; Li, J. Y.; Tung, Y. L.; Wu, C. G. *Dyes Pigm.* **2010**, *84*, 95−101.
(5) Torres, T.; Spanig, F.; Lopez-Duarte, I.; Fischer, M. K. R.; Martinez-Diaz, M. V.; Bauerle, P.; Guldi, D. M. *J. Mater. Chem.* **2011**, *21*, 1395−1403.
(6) Oregan, B.; Gratzel, M. *Nature* **1991**, *353*, 737−740.
(7) Aiga, F.; Tada, T. *Sol. Energy Mater. Sol. Cells* **2005**, *85*, 437−446.
(8) Nazeeruddin, M. K.; Zakeeruddin, S. M.; Lagref, J. J.; Liska, P.; Comte, P.; Barolo, C.; Viscardi, G.; Schenk, K.; Graetzel, M. *Coord. Chem. Rev.* **2004**, *248*, 1317−1328.
(9) Wang, P.; Gao, F. F.; Wang, Y.; Zhang, J.; Shi, D.; Wang, M. K.; Humphry-Baker, R.; Zakeeruddin, S. M.; Gratzel, M. *Chem. Commun.* **2008**, 2635−2637.
(10) Fu, C.; Lei, L.; Sun, K.; Xia, P.; Yuan, H. Y.; Xiao, D.; Li, Z. H. *Renew. Energ.* **2012**, *38*, 163−168.
(11) Han, L. Y.; Numata, Y.; Ashraful, I.; Shirai, Y. *Chem. Commun.* **2011**, *47*, 6159−6161.
(12) Ko, J.; Fang, B. Z.; Fan, S. Q.; Kim, J. H.; Kim, M. S.; Kim, M.; Chaudhari, N. K.; Yu, J. S. *Langmuir* **2010**, *26*, 11238−11243.
(13) Burke, A.; Ito, S.; Snaith, H.; Bach, U.; Kwiatkowski, J.; Gratzel, M. *Nano Lett.* **2008**, *8*, 977−981.
(14) Minaev, B. F.; Baryshnikov, G. B.; A., M. V. *Dyes Pigm.* **2012**, *92*, 531−536.
(15) Li, Y.; Wang, Z.; Zhang, W.; Tao, F.; Meng, K. G.; Xi, L. Y.; Jiang, Q. *Chin. Chem. Lett.* **2011**, *22*, 1001−1004.
(16) Pagani, G. A.; Bagnis, D.; Beverina, L.; Huang, H.; Silvestri, F.; Yao, Y.; Yan, H.; Marks, T. J.; Facchetti, A. *J. Am. Chem. Soc.* **2010**, *132*, 4074−4075.
(17) Yan, Z. Q.; Xu, H. Y.; Guang, S. Y.; Zhao, X.; Fan, W. L.; Liu, X. Y. *Adv. Funct. Mater.* **2012**, *22*, 345−352.
(18) Yan, Z. Q.; Guang, S. Y.; Xu, H. Y.; Liu, X. Y. *Analyst* **2011**, *136*, 1916−1921.
(19) Maeda, T.; Nakao, H.; Kito, H.; Ichinose, H.; Yagi, S.; Nakazumi, H. *Dyes Pigm.* **2011**, *90*, 275−283.

(20) Yum, J. H.; Walter, P.; Huber, S.; Rentsch, D.; Geiger, T.; Nüesch, F.; De Angelis, F.; Grätzel, M.; Nazeeruddin, M. K. *J. Am. Chem. Soc.* **2011**, *129*, 10320−10321.

(21) Maeda, T.; Hamamura, Y.; Miyanaga, K.; Shima, N.; Yagi, S.; Nakazumi, H. *Org. Lett.* **2011**, *13*, 5994−5997.

(22) Jyothish, K.; Avirah, R. R.; Ramaiah, D. *Org. Lett.* **2006**, *8*, 111−114.

(23) Burke, A.; Schmidt-Mende, L.; Ito, S.; Grätzel, M. *Chem. Commun.* **2007**, 234−236.

(24) Frisch, M. J.; Trucks, G. W.; Schlegel, H. B.; Scuseria, G. E.; Robb, M. A.; Cheeseman, J. R.; Montgomery, J. A. J.; Vreven, T.; Kudin, K. N.; Burant, J. C.; et al. *Gaussian 03*, revision A.1; Gaussian, Inc.: Pittsburgh, PA, 2004.

(25) Yao, Q. W.; Kinney, E. P.; Yang, Z. *J. Org. Chem.* **2003**, *68*, 7528−7531.

(26) Geiger, T.; Kuster, S.; Yum, J. H.; Moon, S. J.; Nazeeruddin, M. K.; Grätzel, M.; Nüesch, F. *Adv. Funct. Mater.* **2009**, *19*, 2720−2727.

(27) Wang, Z. S.; Koumura, N.; Cui, Y.; Takahashi, M.; Sekiguchi, H.; Mori, A.; Kubo, T.; Furube, A.; Hara, K. *Chem. Mater.* **2008**, *20*, 3993−4003.

8900

dx.doi.org/10.1021/jp300155g | *J. Phys. Chem. C* 2012, 116, 8894−8900